

A FAST AND SIMPLE METHOD FOR THE VISUAL ENHANCEMENT OF MICROCALCIFICATIONS IN DIGITAL MAMMOGRAMS BASED ON MATHEMATICAL MORPHOLOGY

by

Tomislav M. STOJIC

Faculty of Mechanical Engineering, University of Belgrade, Belgrade, Serbia

Scientific paper
DOI: 102298/NTRP1402108S

A fast and simple method for the visual enhancement of small bright details in digital mammograms based on mathematical morphology is proposed. By a proper choice of the shape and size of the structuring element, an algorithm for a particular processing task – in this case, for the visual enhancement of microcalcifications in digital mammograms – was designed. The efficiency of the proposed algorithm was tested on publicly available mammograms from the mammographic image analysis society database. In all tested cases (23 mammograms), the proposed method successfully segmented and enhanced the existing microcalcifications, independently verified by medical experts. The proposed procedure may be used both as a visual aid in clinical mammogram analysis or as a preprocessing step for further processing, such as segmentation, classification and detection of microcalcifications. Moreover, the algorithm is very fast and robust, thus applicable to real-time mammogram processing.

Key words: mammography, microcalcification, image processing, mathematical morphology, local contrast enhancement

INTRODUCTION

Breast cancer is one of the most frequent malignant diseases in women. A recently published prognosis from the American Cancer Society [1] estimated 232,340 new cases of invasive breast cancer in United States only, as well as 64,640 additional cases of *in-situ* breast cancer. Only lung cancer accounts for more cancer deaths in women in the United States [1]. Breast cancer is also the most common cancer in females in Europe, causing one in six of all deaths from cancers in women [2].

Primary prevention seems impossible since the causes of this disease remain unknown. Thus, an early detection is the key to improving breast cancer survival. The only proven effective method of early detection of breast cancer is mammography [1, 3]. In the final twenty years of the twentieth century, massive breast screening has indeed reduced mortality by up to 30% in western European countries [4]. Conventional screen-film mammography comprises taking an X-ray image of the breast under specific positioning and compression. Upon acquisition, X-ray images are analyzed by experienced radiologists. The latest technology, full-field digital mammography, allows direct

digitalization: the radiology image is converted directly to a digital image, without the use of film. According to the results of the clinical study (involving 387 women and 1548 mammograms), we have come to the conclusion that [5] digital mammography was superior, both in terms of image quality and radiation dose, over screen-film mammography.

The presence of microcalcification clusters is an important sign for the detection of early breast carcinoma. Microcalcifications are small calcium deposits accumulated in breast tissue, appearing as small bright spots on the mammogram image. The small size of microcalcifications (from 50 μm to 1.0 mm, typically 0.3 mm) [3, 4] makes them difficult to detect, requiring expertise by skilled radiologists. As they are often the sole sign of early cancerous changes, microcalcifications represent very important information in a mammogram. The cluster of microcalcifications is the most frequent radiological feature in asymptomatic breast cancer and often leads to surgical biopsy for the establishment of the final diagnosis.

Mammogram analysis is based on the use of different digital image processing techniques aimed at detecting suspicious areas within the breast. Many standard processing methods, such as brightness transformations, contrast enhancement, histogram processing, filtering in spatial and/or frequency do-

* Corresponding author; e-mail: tstoje@mas.bg.ac.rs

main, *etc.* use a set-theory-based approach, *mathematical morphology* [6, 7]. From a practical point of view, morphological operations are recognized as a powerful tool for both image preprocessing, as well as for extracting different image information, such as noise reduction, edge detection, object separation, shape recognition [6, 7], *etc.* Different morphological methods have already proved their efficiency in mammogram segmentation and enhancement of microcalcifications [8-11].

In this paper, the author proposes a fast, simple and efficient method for the visual enhancement of small size bright objects in mammograms, based on mathematical morphology. It will be shown that both local contrast enhancement and high suppression of background tissue can be obtained by combining several morphological operations in an appropriate way. As a result, small details brighter than their surroundings are strongly enhanced. The proposed method is very suitable for extracting and enhancing small bright details (possible microcalcifications) within the X-ray images, since such tissue abnormalities are usually brighter than the background, due to their higher attenuation of the X-rays. The efficiency of the proposed method was tested on publicly available mammograms from the mammographic image analysis society (miniMIAS) database [12].

METHOD DESCRIPTION

Basics of mathematical morphology

Morphological image processing techniques originated from the modern mathematical Set Theory [6, 7]. These morphological operations were originally developed for the analysis of binary (black and white) images, later on extending to monochrome (gray-scale) and multicomponent (color) images. In image processing, all morphological operations are based on the relationships between two particular sets: the first set is represented by an input image matrix, I , while the second one is the processing operator, the so-called structuring element, S . The structuring element also has the matrix form whose dimension is significantly smaller than the size of the input image.

Two morphological operations: *dilation* and *erosion* are fundamental to morphological processing. (In this paper, only the morphological algorithms applied to gray-scale images are considered.)

The dilation of a two-dimensional gray-scale digital image, $I(m, n)$, by a two-dimensional structuring element, $S(i, j)$, is defined as [6, 7]

$$(I \oplus S)(m, n) = \max\{I(m-i, n-j) \mid S(i, j)\} \quad (1a)$$

assuming $[(m-i), (n-j)] \in D_I; (i, j) \in D_S$ where D_I and D_S are the domains of I and S , respectively. The or-

igin of S is assumed to coincide with the actual/current position (m, n) of the input image. Note that for pixels on the boundary of the image, portions of the structuring element may exceed the image area; this is usually compensated by expanding the image with zero values or by an appropriate repetition by pixel values from bordering rows and columns.

From eq. (1a), the pixel at point (m, n) is replaced by the maximum value of per-pixel sums of image pixels and the structuring element within this domain. If all members of a structuring element are positive, the output image tends to be brighter than the input, while the dark details are reduced or completely removed, depending on how their values and shapes relate to the structuring element used.

Very often, the so-called *flat* structuring element (all elements have the same value, usually the value of unity) is used when the dilation can be described as

$$(I \oplus S)(m, n) = \max\{I(m-i, n-j) \mid [(m-i), (n-j)] \in D_I; (i, j) \in D_S\} \quad (1b)$$

This way, the pixel element at point (m, n) is replaced by the maximum value of image pixels covered by the structuring element.

Gray-scale erosion is defined as

$$(I \ominus S)(m, n) = \min\{I(m-i, n-j) \mid S(i, j)\} \quad (2a)$$

assuming $[(m-i), (n-j)] \in D_I; (i, j) \in D_S$ where D_I and D_S are the domains of I and S , respectively. The condition that $(m-i)$ and $(n-j)$ have to be within the domain of I , and i and j have to be in the domain of S , denotes that the structuring element has to be completely contained within the set that is being eroded, *i. e.*, that the structuring element is covered by I . Erosion results in replacing pixel values with the value of the per-pixel difference $(I - S)$ within the domain defined by the size and shape of the structuring element. If all members of the structuring element are positive, the output image tends to be darker than the input. The bright details in the input image are reduced or removed, depending on how their values and shapes relate to the structuring element. As with dilation, when using the flat structuring element, the erosion can be rewritten as

$$(I \ominus S)(m, n) = \min\{I(m-i, n-j) \mid [(m-i), (n-j)] \in D_I; (i, j) \in D_S\} \quad (2b)$$

Several commonly used symmetrical structuring elements such as: cross, square, disk, and rhombus – also known as a diamond, are shown in fig. 1. The dark squares correspond to the values of unity, while the bright ones denote zero-valued elements.

The size and shape of a structuring element play a crucial role in morphology-based image processing

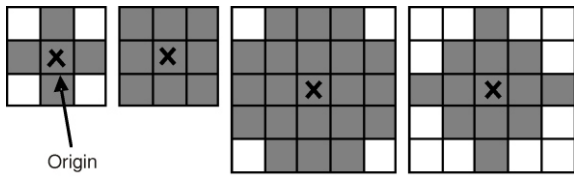


Figure 1. Several symmetrical structuring elements; from left to right: cross (3 3), square (3 3), disk (5 5), and diamond (5 5); the origin (center) of each element is marked by *x*

since they define the neighborhood used for processing the currently analyzed pixel.

By combining the two basic morphological operations, described by eqs. (1) and (2), one can derive useful operations conceptually similar to those with two-dimensional (2-D) filters. For example, *morphological gradient G* is the difference between dilation and erosion

$$G = (I \circ S) - (I \oslash S) \quad (3)$$

Since dilation and erosion remove the small, dark and bright details, respectively, the morphological gradient highlights sharp gray-level transitions in the input image.

The next two morphological operations of interest are *opening* and *closing*. The opening of an image *I* by a structuring element *S* is defined as erosion followed by dilation, while closing has the opposite order of operations

$$I \circ S = (I \oslash S) \circ S, \text{ opening} \quad (4)$$

$$I \oslash S = (I \circ S) \oslash S, \text{ closing} \quad (5)$$

as a consequence, with a gray-scale opening, one can remove bright details smaller than the structuring element used. Large details, both bright and dark, which are larger than the structuring element, remain nearly unchanged. Similarly, the closing operation removes dark details if they are smaller than the structuring element.

By combining the morphological opening and closing, various image-processing tasks can be performed. For instance, a *smoothing* effect is obtained with a morphological opening followed by a closing. As a result, both bright and dark pixels with intensities significantly different from their surroundings will be removed or attenuated and the output image smoothed.

The following two morphological operations are the so-called *top-hat (TH)* and *bottom-hat (BH)* transformations. A *top-hat* transformation is obtained by subtracting a morphologically opened image from the original one

$$TH = I - (I \circ S) \quad (6)$$

As already mentioned, a gray-scale opening can remove the bright details from an input image smaller

than the used structuring element. Subtracting an opened image from the original one yields an image with emphasized details which are suppressed by the opening. Thus, *TH* transformation is an excellent tool for enhancing small bright details from a non-uniform background [7].

The morphological *bottom-hat* transformation is defined as the difference between a morphologically closed image and the original one

$$BH = (I \oslash S) - I \quad (7)$$

Consequently, this transformation produces an effect opposite to the *top-hat* transformation. This means that, by using closing instead of opening, and by subtracting the original image from the closed one, one can extract dark features from a brighter background. Note that both transformations equalize a non-uniform background illumination.

Morphological reconstruction is a transformation involving two images and a structuring element (instead of a single image and a structuring element) [13]. One image, the marker, is the starting point for the transformation. The second image, the mask, constrains the transformation. The structuring element *S* defines the connectivity (8- and 4-connectivity are usually used). The eight-connectivity implies that *S* is a square 3 3 matrix of 1 s, with the center defined at co-ordinates (2, 2), corresponding to the “square” case shown in fig. 1. Similarly, 4-connectivity corresponds to the “cross” case in the same figure. If *I* is the mask and *J* is the marker, the reconstruction of *I* from *J*, denoted as $R_I(J)$, is defined by the following iterative procedure [13]:

- initialize H_1 to be the marker image, *J*,
- define connectivity by structuring element *S*,
- repeat: $H_{k+1} = (H_k \oslash S) \circ I$, until $H_{k+1} = H_k$, and
- $R_I(J) = H_{k+1}$

Symbols \circ and \oslash denote the operations of intersection and dilation, respectively. Note that the marker image *J* must be a subset of mask image *I*, $J \subseteq I$, i. e., that the gray level of each pixel in *J* must be less than or equal to the gray level of the corresponding pixel in *I* image. Although this iterative formulation is conceptually useful, much faster computational algorithms exist [14]. This transformation preserves only those objects in the mask image which are pointed by markers from the marker image, forming the basis for many other complex morphological transformations [6, 7, 13].

A useful application of this reconstruction is the removal of objects that touch the border of an image. Here, the key task is to select the appropriate marker image to achieve the desired effect. Let mask image *I* be the input image and marker image *J* be zero everywhere except along the input image border where it equals the input image *I*. Thus, using input image *I* as the mask image, the reconstruction $H = R_I(J)$ yields image *H* that contains only the objects touching the border. The difference

$$I \ominus I \oplus H \ominus I \oplus R_I(J) \quad (8)$$

will contain only those objects from the original input image that do not touch the border. In this way, one can suppress structures that are brighter than their surroundings and connected to the image border. Note that this “image border clearing” tends to reduce the overall gray level intensity of the image.

Local contrast enhancement

High local contrast enhancement can be achieved by adding an original image to the *top-hat* transformed image and by subtracting the *bottom-hat* image from that sum

$$C = (I \oplus TH) \ominus BH \quad (9)$$

Due to this difference, bright details smaller than the structuring element are strongly emphasized, while dark details and the overall image texture surrounding the small bright details are suppressed. Consequently, the enhancement of bright details smaller than the structuring element S is being reinforced, while the uneven background (surrounding tissue texture) is highly equalized. Further on, by applying the “image border clearing” transformation, eq. (8), onto the contrast-enhanced image C , eq. (9), by substituting $I = C$, one can suppress bright structures around the image border regardless of its shape and dimensions and, at the same time, reduce the overall brightness of the processed image. This is very useful because the objects of interest, microcalcifications, are not located around the image border; instead, some other bright structures close to the border, such as the pectoral muscle or other markers are to be found there. In addition, reducing overall image brightness helps in preventing the possible premature saturation of pixel's graylevel after applying the operation described by eq. (9).

The described procedure can be iteratively repeated by using the output image from the k -th iteration as the input image for the next one, $(k + 1)$ -th, iteration, *i. e.*, by applying

$$I^{(k+1)} = C^{(k)}, k = 1, 2, 3, \dots \quad (10)$$

and, by repeating the procedure described by eqs. (8)-(10). The proposed method converges very fast. Intensive simulations showed that no more than two iterations are sufficient. The transformed image contains only small bright details, while uneven background tissue is highly equalized.

By an appropriate selection of the shape and size of the structuring element, as well as the number of necessary iterations, the proposed algorithm may be customized to particular processing tasks.

Procedure for the extraction and visualization of microcalcifications in mammograms

The described morphological method for local contrast enhancement was applied to the extraction and visualization of microcalcifications in digital mammograms. Assuming the most likely structure of microcalcifications [4] and their main features observed in digital images [15, 16], the disk-shaped structuring element was selected for their enhancement. The size of the structuring element depends on the expected dimensions of microcalcifications and the spatial resolution of the digital mammogram.

Before applying the algorithm, the mammograms were preprocessed to extract the breast tissue region from the mammograms. Initially, the original mammogram is converted to a binary (black and white) image, by thresholding following the Otsu method [17]. After that, the obtained binary image is *flood-filled* [6] to remove isolated black pixel islands within the segmented white regions. In addition, the small details outside the breast region (such as labels) are removed using an opening with a large structuring element. The resulting image is then segmented into connected components, using 8-connectivity. The connected component with the largest number of pixels (corresponding to the breast tissue region) is declared as the region of interest (ROI). All further processing is applied only to the image pixels within the ROI.

The iterative procedure for local contrast enhancement described in eqs. (8)-(10) starts with the structuring element size close to the expected upper limit of the microcalcification's dimension (about 2 mm) [3, 4, 11]. The size of the structuring element appropriately decreases with subsequent iteration since, once finding the possible microcalcification, the method tries to detect its peak, or dome [6, 14, 15].

The final segmentation of microcalcifications is obtained by thresholding applied to the k -th output image $C^{(k)}$. First, the magnitudes of all pixel values in the output image are normalized, which leads to the new image with pixel values within the range [0-1]. After that, by choosing the proper threshold value, T , one can extract the bright details (microcalcification candidates) from the background. Any pixel with a gray level L larger than T is labeled as white (corresponding normalized value = 1), while other pixels are labeled as black (normalized value = 0). In this manner, the extracted details are presented as white islands within a black surrounding. The contour lines of the segmented bright objects may be extracted and superimposed onto the original mammogram so as to further help radiologists. This thresholding procedure is performed in an interactive manner, allowing the adjustment of threshold level T for finding the best result. In addition, shape parameters (such as area, eccentricity, diameter ...) of segmented objects (enclosed by contour lines) may be

easily measured [10] and further used for their description and classification. As with any other measuring procedure, measurement uncertainty should be taken into account with great care [18].

It has to be said that not all details extracted in this manner necessarily correspond to microcalcifications. The proposed method enhances all details brighter than the background and smaller than the structuring element used. Among the desired parts (microcalcifications), such details may be film artifacts, noise, *etc.* The removal of these details can be carried out by the postprocessing of the segmented image. For example, film emulsion artifacts are seen as isolated bright spots (one or two pixels wide) in a mammogram. These artifacts can be removed by opening the segmented image with a small structuring element of a radius equal to only two pixels.

RESULTS

The proposed algorithm has been tested using publicly available mammograms from the miniMIAS database [12]. The database includes a total of 23 mammograms with clinically approved microcalcifications. In all of the cases, the proposed method successfully enhanced the existing microcalcifications. The efficiency of the method can be illustrated by observing three characteristic examples from the miniMIAS database.

All mammograms in the miniMIAS database are of 1024 × 1204 pixels size, 8 bits per-pixel gray-level depth, *i. e.*, having gray-levels from 0 (black) to 255 (white), and with a 200 μm spatial resolution. Under these circumstances, the algorithm for local contrast enhancement has incorporated the structuring element of a radius $R = 5$ pixels (corresponding to the microcalcification diameter of 2.2 mm). Intensive simulations showed that two iterations are sufficient for achieving convergence. For the second iteration, the radius of the structuring element was decreased to $R = 4$ pixels.

For a better visualization of details, all figures in this paper are depicted after contrast stretching: the actual gray-level range from $L_{\min} > 0$ to $L_{\max} < 1$ is extended to full range, [0-1].

First case: In fig. 2(a), a mammogram, mdb249.pgm, from the miniMIAS database is depicted. The microcalcifications (verified and marked by radiology experts) are located within the solid white rectangle.

Figure 2(b) shows the output image $C^{(2)}$ obtained by applying the iterative procedure described by eqs. (8)-(10), after second iterations. Note that the iterative image processing is performed using only the pixels within the ROI (segmented breast tissue region). The microcalcifications are accentuated, while the surrounding tissue is suppressed. In fig. 2(c) the output result obtained after applying the method is depicted. The microcalcifications' contour lines are embedded in the original image. Microcalcifications marked by experts from the MIAS society were then

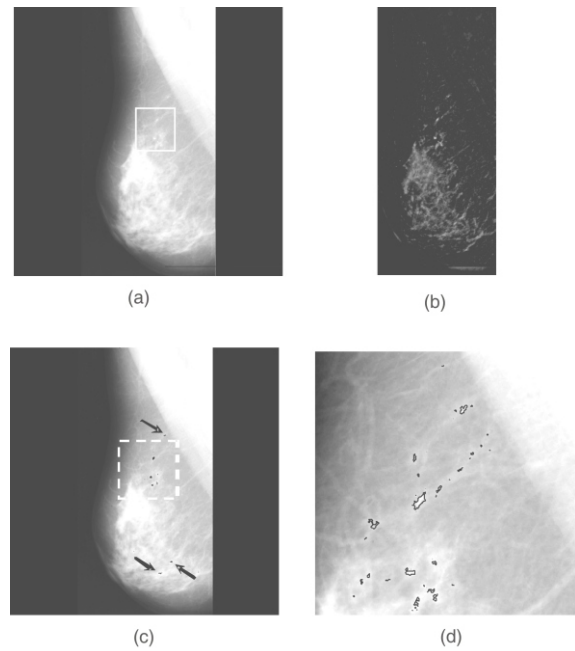


Figure 2. (a) mammogram mdb249.pgm – the cluster of approved microcalcifications is within the white rectangle; (b) transformed image $C^{(2)}$ after 2 iterations; (c) mammogram mdb249.pgm with superimposed microcalcifications' contour lines (threshold $T = 0.4$) – black arrows indicate to segmented objects outside the declared region; (d) zoomed detail (size: 256 × 256 pixels), corresponding to the white dashed rectangle from fig. (c)

segmented by using the proposed method. However, the said method extracted even some details outside the declared cluster of microcalcifications, probably corresponding to the isolated microcalcifications indicated by black arrows in fig. 2(c). For better visualization, a zoomed detail (size: 256 × 256 pixels) around the cluster of microcalcifications is presented in fig. 2(d).

Second case: The example in fig. 3(a) corresponds to the mammogram (mdb256.pgm) from the miniMIAS database. The cluster with verified microcalcifications is located within the solid white rectangle. In this case, the breast tissue is predominantly fatty. Visual detection of microcalcifications is difficult due to the poor contrast between microcalcifications and surrounding tissue.

The transformed image of the breast region in the mammogram after two iterations, $C^{(2)}$, is shown in fig. 3(b). The background texture is homogenized, the pectoral muscle removed almost completely and only small details brighter than the surrounding tissue are enhanced. In fig. 3(c), the original mammogram with the superimposed contour lines around the enhanced microcalcifications is shown. Contour lines are extracted from the normalized image $C^{(2)}$ by applying the threshold of $T = 0.65$. As in the previous case, the proposed method detected some other objects outside the

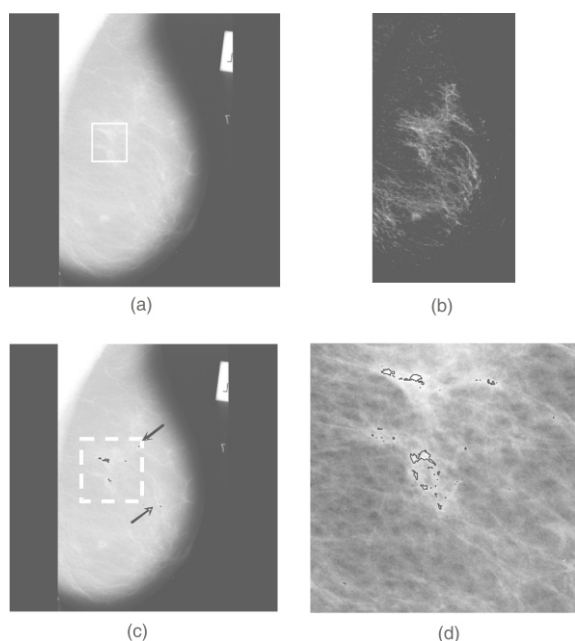


Figure 3. (a) mammogram mdb256.pgm – the position of approved microcalcifications is labeled by the white rectangle; (b) transformed image $C^{(2)}$ after 2 iterations; (c) mammogram mdb56.pgm with superimposed microcalcifications' contour lines (threshold $T = 0.65$) – black arrows indicate to segmented objects outside the declared region; (d) zoomed detail (size: 256×256 pixels), corresponding to the white-dashed rectangle in fig. (c)

declared cluster of microcalcifications, indicated by black arrows in fig. 3(c). In fig. 3(d), a part of the original mammogram (256×256 pixels), corresponding to the dashed white rectangle from fig. 3(c) with superimposed contour lines around segmented microcalcifications, is depicted.

Third case: Mammogram mdb241.pgm from the miniMIAS database is shown in fig. 4(a). The verified microcalcifications are located within the white solid rectangle.

In this case, the breast tissue is dense, causing a very poor contrast between microcalcifications and the surrounding tissue. Consequently, the visual detection of microcalcifications is very difficult even for skilled radiologists. But, after applying thresholding on the morphologically enhanced $C^{(2)}$ image after two iterations, microcalcifications may be extracted, as shown in fig. 4(b). The contour lines are obtained after applying the threshold of $T = 0.5$. For better visualization, the zoomed detail 256×256 pixels corresponding to the white-dashed rectangle in fig. 4(b) is depicted in fig. 4(c).

CONCLUSIONS

A fast, simple and efficient method for enhancing small bright details in digital mammograms, based on mathematical morphology, is proposed.

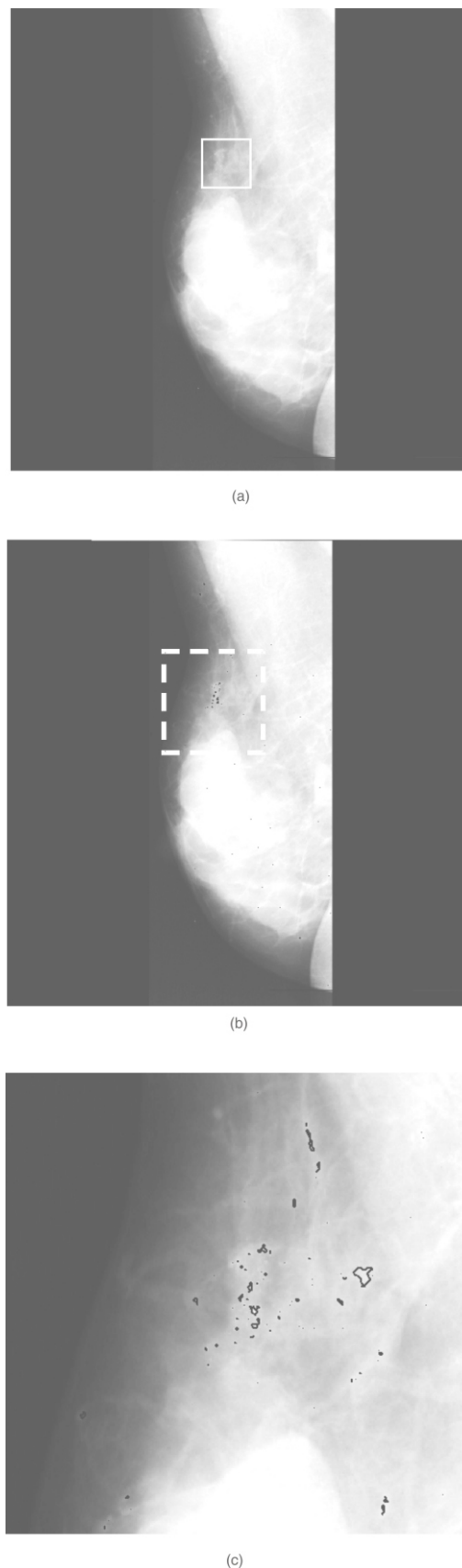


Figure 4. (a) mammogram mdb241.pgm. – inside the solid white rectangle is the cluster with verified microcalcifications; (b) mammogram mdb241.pgm with the superimposed microcalcifications contour lines (threshold $T = 0.5$); (c) zoomed detail (256×256 pixels), corresponding to the white-dashed rectangle in fig. (b)

Work has also shown that high local contrast enhancement, followed by the suppression of surrounding tissue, may be achieved by using an appropriate combination of certain basic morphological transformations. Iterative application of the proposed method highly enhances small, bright details, suppressing the background tissue. This is suitable for mammogram analysis since microcalcifications, often the sole early breast cancer signs, are usually displayed in the form of bright details in a mammogram, due to their high attenuation of X-rays. The simulation of the proposed method suggests that two iterations are sufficient for extracting the desired details. The final segmentation is obtained by thresholding the processed output image. By an appropriate choice of the threshold, one can extract the desired bright details from the background and then segment their contour lines. By superimposing contour lines onto the original mammogram, the visualization of the segmented bright details is highly improved. The said procedure can be performed in an interactive manner, so as to allow for the adjustment of the threshold level for attaining best results. By a proper choice of the shape and size of the structuring element, the proposed algorithm can be customized to a particular processing task.

Work has focused on the segmentation and visualization of microcalcifications in digital mammograms. Based on the expected structure of microcalcifications [4], the disk-shaped structuring element was selected. The size of the structuring element depends on the expected upper limit of microcalcifications dimension (about 2 mm) and on the spatial resolution of digital mammograms.

The application of the algorithm was tested by using publicly available mammograms from the miniMIAS [12] database. In all 23 tested cases, the proposed method successfully extracted microcalcifications, previously indicated by a radiologist. Moreover, the algorithm is fast and computationally simple and, thus, appropriate for realtime mammogram processing. The procedure could be used both as a visual aid in mammogram analysis and as a preprocessing stage for further image processing.

ACKNOWLEDGEMENT

I would like to acknowledge my sincere gratitude to my thesis adviser, Dr. Branimir Reljin (School of Electrical Engineering, University of Belgrade), for the guidance and support given in the preparation and completion of this work.

REFERENCES

- [1] ***, American Cancer Society: Breast Cancer Facts and Figures, <http://www.cancer.org/>, (last visited 2014)
- [2] ***, Health Statistics – Atlas on Mortality in the European Union, (2009 edition), <http://epp.eurostat.ec.europa.eu>

- [3] Sakka, E., Prentya, A., Kotsourise, D., Classification Algorithms for Microcalcifications in Mammograms (Review), *Oncology Reports*, 15 (2006), 4, pp. 1049-1055
- [4] Suri, J., Setarehdan, S., Singh, S., Advanced Algorithmic Approaches to Medical Image Segmentation, Springer-Verlag, 2002
- [5] Stantić, T., *et al.*, Screen-Film vs. Full-Field Digital Mammography: Radiation Dose and Image Quality in a Large Teaching Hospital, *Nucl Technol Radiat*, 28 (2013), 4, pp. 398-405
- [6] Soille, P., Morphological Image Analysis: Principles and Applications (2nd ed), Springer-Verlag, 2003
- [7] Gonzales, R., Woods, R., Digital Image Processing (3rd ed.), Prentice Hall, New Jersey, 2008
- [8] Betal, D., Roberts, N., Whitehouse, G. H., Segmentation and Numerical Analysis of Microcalcifications on Mammograms Using Mathematical Morphology, *The British Journal of Radiology*, 70 (1997), 837, pp. 903-917
- [9] Rangayyana, R., Ayresa, F., Desautels, L., A Review of Computer-Aided Diagnosis of Breast Cancer: Toward the Detection of Subtle Signs, *Journal of the Franklin Institute*, 344 (2007), 3-4, pp. 312-348
- [10] Reljin, B., *et al.*, Computer Aided System for Segmentation and Visualization of Microcalcifications in Digital Mammograms, *Folia Histochemica et Cytobiologica*, 47 (2009), 3, pp. 525-532
- [11] Stojić, T., Reljin, B., Enhancement of Microcalcifications in Digitized Mammograms: Multifractal and Mathematical Morphology Approach, *FME Transactions*, 38 (2010), 1, pp. 1-10
- [12] Suckling, J., The miniMIAS Database, Mammo-graphic Image Analysis Society – MIAS, www.wiau.man.ac.uk/services/MIAS/MIAScom.html
- [13] Gonzalez, R., Woods, R., Eddins, S., Digital Image Processing Using MATLAB (2nd ed), Gatesmark Publishing, 2009
- [14] Vincent, L., Morphological Grayscale Reconstruction in Image Analysis: Applications and Efficient Algorithms, *IEEE Transactions on Image Processing*, 2 (1993), 2, pp. 176-201
- [15] Carton, A-K., *et al.*, Development and Validation of a Simulation Procedure to Study the Visibility of Microcalcifications in Digital Mammograms, *Med. Physics*, 30 (2003), 8, pp. 2234-2240
- [16] Bakić, P., *et al.*, Mammogram Synthesis Using a 3-D Simulation. II. Evaluation of Synthetic Mammogram Texture, *Medical Physics*, 29 (2002), 9, pp. 2140-2151
- [17] Otsu, N., A Threshold Selection Method from Gray-Level Histograms, *IEEE Trans. on System, Man, and Cybernetics*, 9 (1979), 1, pp. 62-66
- [18] Osmokrović, P., Stanković, K., Vujisić, M., Determination of Measurement Uncertainty (in Serbian), Akademska Misao, Belgrade, 2009

Received on March 2, 2104

Accepted on April 17, 2014

Томислав М. СТОЈИЋ

**БРЗА И ЈЕДНОСТАВНА МЕТОДА ЗА ВИЗУЕЛНО ИСТИЦАЊЕ
МИКРОКАЛЦИФИКАЦИЈА У ДИГИТАЛНОМ МАМОГРАМУ
ЗАСНОВАНА НА МАТЕМАТИЧКОЈ МОРФОЛОГИЈИ**

У раду је предложен брз и једноставан алгоритам за визуелно истицање малих светлих детаља у дигиталном мамограму применом методе математичке морфологије. Оптималним избором облика и величине структурног елемента, предложени алгоритам се може брзо прилагодити конкретном задатку – у овом случају визуелном истицању микрокалцификација у дигиталном мамограму. Ефикасност предложеног алгоритма је тестирана коришћењем јавно доступних мамограма из референтне миниМИАС базе. У сва 23 тестирана мамограма из миниМИАС базе са микрокалцификацијама предложена метода је успешно истакла постојеће микрокалцификације. Развијени алгоритам је брз, робустан и погодан за анализу мамограма у реалном времену. Предложена метода може да се користи за визуелну асистенцију у клиничкој анализи мамограма, или у фази претпроцесирања при даљој обради мамограма у циљу сегментације, класификације и детекције микрокалцификација.

Кључне речи: мамографија, микрокалцификација, обрада слике, математичка морфологија, повећање локалног контраста
